Journal of Physical and Theoretical Chemistry
of Islamic Azad University of Iran, 14 (2) 165-177: Summer 2017
(J. Phys. Theor. Chem. IAU Iran)
ISSN 1735-2126

Theoretical studies on corrosion inhibition of N-aroyl-N'-aryl thiourea derivatives using conceptual DFT approach

Semire Banjo* and Oyebamiji Abel Kolawole

Department of Pure and Applied Chemistry, Ladoke Akintola University of Technology, PMB 4000, Ogbomoso, Nigeria

Received November 2017; Accepted December 2017

ABSTRACT

In this paper, quantum chemical parameters at density functional theory (DFT) B3LYP/6-31G** (d,p) level of theory were calculated for three organic corrosion inhibitors [N-benzoyl-N-(p-aminophenyl) thiourea, N-benzoyl-N-(thiazole) thiourea and N-acetyl-N-(dibenzyl) thiourea. The calculated molecular descriptors such as the HOMO, LUMO, dipole moment, chemical potential (μ), chemical hardness (η), global nucleophilicity (ω) and average electronic charges on nitrogen atoms were explained in line with the experimental observed inhibitory efficiency for the compounds. The calculated results revealed that electron density on the rings (Q_{ring} (e)) and thiocarbonyl sulphur atom (S* in C=S) are strongly correlated to the observed %IE. Therefore, electronic interactions such as π-cationic and n-cationic interactions between the molecules and metal surface played prominent roles in adsorption process than electron donor-acceptor model as early reported by Uday et al., 2013 [19].

Keywords: Thiourea derivatives; Molecular descriptors; DFT-QSAR

INTRODUCTION

Research on corrosion inhibition with the aid of organic inhibitors has drawn the attention many researchers because of pivotal roles metal especially iron play in industry [1]. Corrosion as an electrochemical technique steadily converts metal to a more chemically stable form as oxides, hydroxide or sulphide in the milieu is triggered by acid wash, engraving and/or prickling [2]. It gradually reduces the quality and strength of a metal for industrial uses; and this process is usually stark to the carbon steel while in use. Corrosion of metals causes a danger to the humanity as well as the surroundings [3].

Carbon steel, a common metal that is important in engineering works is a metal alloy enclosed the mixture of two major elements, iron and carbon coupled with other small elements such as copper (0.60 %), manganese (1.65%) and Silicon (0.60 %) which are not sufficient to affect its properties. Although, carbon steel possesses outstanding mechanical property, low cost, high strength, availability and ease of fabrication which makes it to be admired in industrial use [4-6]. It is very important in constructions such as bridges, erection of buildings, conduits, heavy vehicles and many other uses [7-9], but it is easily corroded in moist

*Corresponding author: bsemire@lautech.edu.ng

and acidic environments which are activated by acid wash, engraving and/or prickling of the metal surface.

However, introduction of inhibitors are initiated to reduce the corrosion rates of metallic materials. Different groups of organic compounds have been reported to exert inhibitive effects on the corrosion of mild steel especially compounds that contain heteroatoms (i.e. nitrogen, oxygen, sulphur) via adsorption on the metal surface [10]. The adsorption of organic compounds containing heteroatoms on metal surface serves as the first step of inhibition. The adsorption of organic inhibitors on metal surface is controlled by the physico-chemical properties of the molecule such as functional group, steric factor, molecular size, electron density at the atoms that donates and π-orbital character of donating electrons. In addition, ability of the inhibitor to accept free electrons from unoccupied d-orbital of the metallic surface by using their anti-bonding orbital to form feedback bonds is also very essential [11-14].

Furthermore, the use of quantum chemical calculations in elucidating physical characters that take part in the inhibition has turn out to be a recognizing and popular phenomenon in the study of corrosion inhibition [15]. More so, density functional theory (DFT) methods have been a veritable tool for examining several derivatives of organic inhibitors in order to correlate their molecular properties to their inhibitory efficiencies as a better way to design inhibitors with improved efficiencies. Recently, with the aid of density functional theory, selection of inhibitors are emphasized via comparing the experimental data to calculated molecular descriptors such as HOMO, LUMO, binding energy dipole moment, charges on every heteroatoms [16-19].

NPT

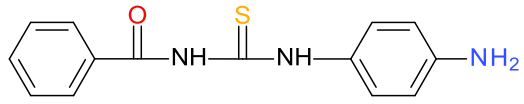

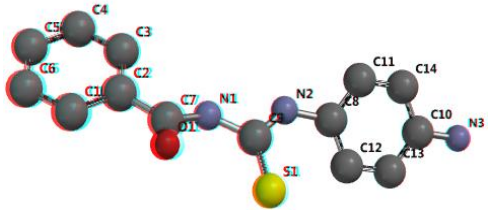

N-benzoyl-N-(p-aminophenyl) thiourea (**NPT**)

NTT

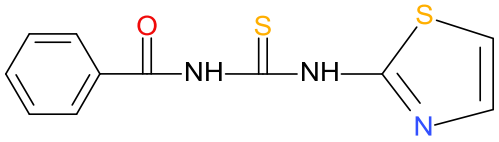

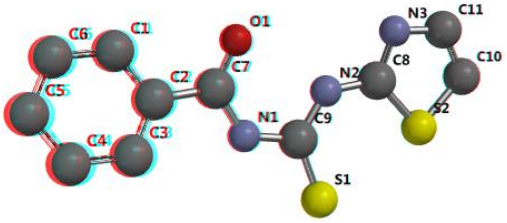

N-benzoyl-N-(thiazole)thiourea (**NTT**)

NDT

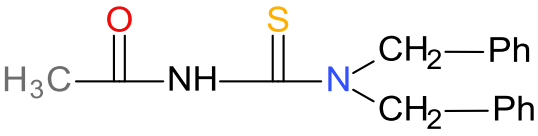

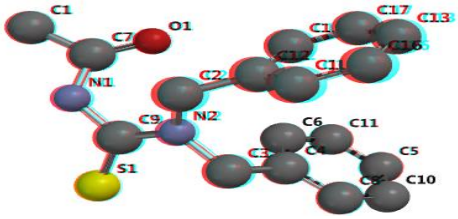

N-acetyl-N-(dibenzyl)thiourea (**NDT**)

Figure 1. Schematic and optimized structures with numbering of the examined compounds.

Additionally, the calculated molecular properties are always related to the observed activity of the compounds in order to predict quantitatively the activity of similar compounds known as quantitative structural activity relationship (QSAR). The QSAR embroils the arithmetical formula which relates the inhibitory activities of a group of molecules to their calculated molecular descriptors [20]. The QSAR has characteristically achieved eclectic applicability for relating molecular descriptors with not only inhibitory activities but also with other physicochemical properties. Therefore, establishment of dependable QSAR model play an important role in the inhibitory process [21].

Therefore, in this paper, quantum chemical calculations would be performed on three compounds i.e. N-benzoyl-N-(p-aminophenyl) thiourea (NPT), N-benzoyl-N-(thiazole)thiourea (NTT) and N-acetyl-N-(dibenzyl)thiourea (NDT) as shown in Figure 1. The molecular parameters calculated are correlated to the observed inhibitory activities for the compounds. Thus, the major aim of this work is to use conceptual density functional theory (DFT) method to calculate molecular descriptors and relate the calculated parameters to the experimentally observed inhibition efficiencies of thiourea derivatives as well as establishing QSAR model from the calculated descriptors that could predict the experimental inhibition efficiencies. The thiourea derivatives used in this paper have been examined experimentally their corrosion inhibition efficiency by Uday et al., 2013 [22].

COMPUTATIONAL DETAILS

Firstly, Conformational search was carried out on N-benzoyl-N-(p-aminophenyl) thiourea (NPT), N-benzoyl-N-(thiazole)thiourea (NTT) and N-acetyl-N-(dibenzyl)thiourea (NDT) using semi-empirical AM1 method Monte Carlo search algorithm. 500 conformers were examined for each compound; only conformers within ±5 Kcal/mol of energy window were considered and the lowest-energy conformer of his conformational search was taken for DFT calculations [23]. The full optimization of the lowest-energy conformers for NPT, NTT and NDT were carried out at Density functional theory (DFT) with the standard 6-31G (d, p) basis set. There are three-parameter embedded in DFT; this are Becke's gradient exchange correction and the Lee, Yang, Parr correlation functional (i.e. B3LYP) [24-26]. Single point calculations were performed in aqueous medium at the same level of theory using optimized geometry obtained in the gas phase. The molecular descriptors calculated were chemical hardness (η), chemical softness (S), energies of frontier orbitals (HOMO and LUMO), dipole moment, electronegativity (χ), electrophilicity index (ω), chemical potential (μ) and Funki indices. Therefore, the studied molecules as shown in Figure 1 were gotten from the manuscript written by Uday et al., 2013 [22] and were optimized in order to calculate the parameters that explain the inhibition efficiency [27]. The chemical potential and electronegativity are related as:

$$\boldsymbol{\chi} = \frac{\partial E}{\partial n} V(r) = -\mu = \frac{\boldsymbol{IP+EA}}{\mathbf{2}} = -\left(\frac{\boldsymbol{E_{HOMO}+E_{LUMO}}}{\mathbf{2}}\right) \quad \textbf{(1)}$$

E: is the total energy, μ: chemical potential, *N*: number of electrons and *V*(*r*): external potential of the system.

Also chemical hardness (η) is defined within the DFT as the second derivative of the energy (*E*) with respect to (*N*) as *V*(*r*)

property which measures both stability and reactivity of the molecule as:

$$\eta = \frac{\partial^2 E}{\partial^2 n} V(r) = \frac{\boldsymbol{IP-EA}}{\boldsymbol{2}} = \frac{\boldsymbol{E_{LUMO}-E_{HOMO}}}{\boldsymbol{2}} \quad (2)$$

where *IP*: is the requisite quantity of energy to confiscate one electron from each atom in a mole of gaseous atom to produce one mole of gaseous ion with positive charge in the molecule, which is termed ionization potential. This is approximate to $-E_{HOMO}$; and *EA*: is the energy change that occurs when a gaseous atom acquires an electron to form a univalent negative ion, which is termed electron affinity, this is approximate to $-E_{LUMO}$ [28-31].

The global electrophilicity (ω) and number of electrons transfer (ΔN) are calculated using $\omega = \frac{\mu^2}{2\eta}$ (3) and $\Delta N = \frac{\chi_{Fe}-\chi_{inh}}{2(\eta_{fe}-\eta_{inh})}$ (4) respectively.

where χ_{Fe} and χ_{inh} are absolute electronegativity of the metal (Fe) and inhibitor molecule respectivity, η_{Fe} and η_{inh} are the absolute hardness of iron and the inhibitor molecule respectively. The value of χ_{Fe} is taken to be = 7.0 eV and η_{Fe} = 0 for the computation electron transferred.

The simple charge transfer model for donation and back-donation of charges proposed by Gomez et al., [32], an electronic back-donation process which might be to govern the interaction between the inhibitor molecule and the metallic surface. This model establishes that the energy change involves charge transfer to the molecule and back-donation from the molecule is directly related to the hardness of the molecule as shown in equation 5.

$$\Delta E_{\text{Back-donation}} = -\frac{\eta}{4} \quad (5)$$

The $\Delta E_{\text{Back-donation}}$ implies that when $\eta > 0$ and $\Delta E_{\text{Back-donation}} < 0$, the charge transfer to a molecule, followed by a back-donation from the molecule, is energetically favored. Thus, the stabilization among inhibiting molecules interacting with the same metal surface can be compared. It is expected that $\Delta E_{\text{Back-donation}}$ will decrease as the hardness increases.

The Local reactivity indices which are used to elucidate the reactivity of specific atom in a molecule in relation to the adsorption of an organic inhibitor on a specific metallic surface. However, the variation in electron density for a nucleophile $f^{+}_{(r)}$ and $f^{-}_{(r)}$ as the Funki functions which can be calculated by the finite differences approximation [33];

$f_k{}^{+}_{(r)} = q_kN+1_{(r)} - q_kN_{(r)}$ (for nucleopilic attack) (5)

$f_k = q_kN_{(r)} - q_kN\text{-}1_{(r)}$ (for electrophilic attack) (6)

where $q_kN+1_{(r)}$, $q_kN_{(r)}$ and $q_kN\text{-}1_{(r)}$ are the electronic densities of anionic, neutral and cationic species respectively.

Finally, a statistical method of analysis via multiple linear regression (MLR) is used to develop a model that correlates molecular properties to the inhibitory activity these compounds known as quantitative structure-activity relationship (QSAR). The model was verified for practical suitability by using statistical parameters like correlation coefficient (r), cross validation (R^2) and adjusted as shown is equations (6) and (7). The evaluated QSAR model was used to use to predict the corrosion inhibitory activity of the N-Aroyl-N-Aryl thiourea derivatives.

$$CV.R^2 = 1 - \frac{\sum(\gamma_{obs}-\gamma_{cal})^2}{\sum(\gamma_{obs}-\bar{\Upsilon}_{obs})^2} \quad (6)$$

The R^2 adjusted could be calculated using equation (7)

$$R_a^2 = \frac{(N-1)\times R^2 - P}{N-1-P} \quad (7)$$

So, the QSAR model could be considered prognostic, if R^2_{pred} > 0.6.

RESULTS AND DISCUSSION

Quantum chemical molecular descriptors

In this research work, the calculated molecular descriptors are solvation energy, weight, hydrophobicity (Log P), volume (V), Area, polar surface area (PSA), ovality, dipole moment (DM), heteroatoms (average of Mulliken charges on all heteroatoms), highest occupied molecular orbital (HOMO), and lowest occupied molecular orbital (LUMO) energies as shown in Table 1. Both the HOMO and LUMO are very important parameters which give convincing qualitative information about the excitation properties i.e. the HOMO provides information about the regions in the molecule which has the most energetic electrons and these electrons are bequeathed to the electron poor species. Similarly, the LUMO is an orbital which has the lowest energy offers information on the areas in a molecule that possess the utmost propensity to accept electrons from an electron rich species [19, 34-35]. Therefore, the calculated HOMO energies for the compounds are -5.23, -6.03 and -5.77eV for **NPT, NTT** and **NDT** respectively. It is expected that **NPT** with highest HOMO energy will donate electrons to the metal surface than **NTT** and **NDT;** therefore, behave/serve as a better corrosion inhibitor as well as an ideal inhibitor in the sequence. Nevertheless, as shown in Table 1 **NDT** appeared to be a better corrosion inhibitor (%I.E = 95.49). Therefore, the trend in HOMO energies was not agreed with the observed corrosion inhibition efficiencies of the compounds. The LUMO energy (E_{LUMO}) is calculated to be -1.48eV for **NPT**, -2.11eV for **NTT** and -1.11eV for **NDT**; this means **NTT** with lowest E_{LUMO} will be readily inhibitor to accept electrons from d-orbital of corroding metal.

The energy band gap between HOMO-LUMO energy levels (Band gap) is another vital descriptor that is needed to be put into consideration; since the smaller the band gap, the greater the corrosion inhibition efficiency [36]; Binding ability of the inhibitor to the metal surface increases with increasing of the HOMO and decreasing of the LUMO energy values [37]. However, the calculated band gap is inversely correlated to the observed % IE, this suggests that aromaticity in terms of π-interactions of the inhibitors play a crucial role in adsorption process on metal surface.

Table 1. Selected molecular parameters obtained by B3LYP/6-31G**

Mol	HOMO (eV)	LUMO (eV)	M (eV)	ω (eV)	Het (*e*)	ΔN	%IE
NPT	-5.23	-1.48	-3.36	3.00	-1.26	0.971	79.12
NTT	-6.03	-2.11	-4.07	4.22	-0.99	0.747	81.82
NDT	-5.77	-1.11	-3.44	2.54	-1.53	0.764	95.49

MW = Molecular weight, Het = average electronic charges on heteroatoms, %IE = inhibition efficiency

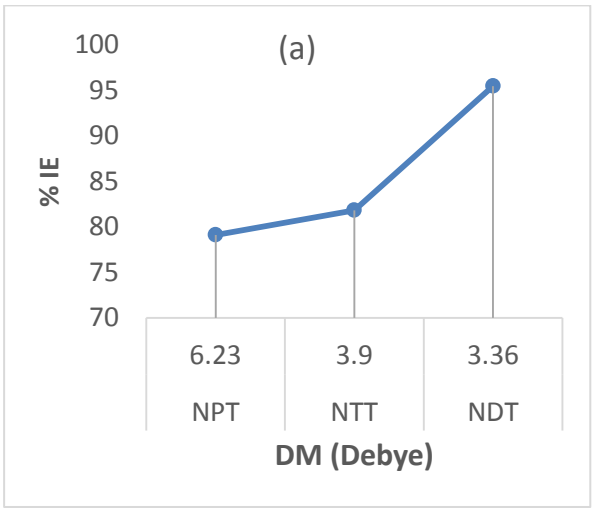
(a)
100
95
90
85
80
75
70
% IE
6.23
3.9
3.36
NPT
NTT
NDT
DM (Debye)

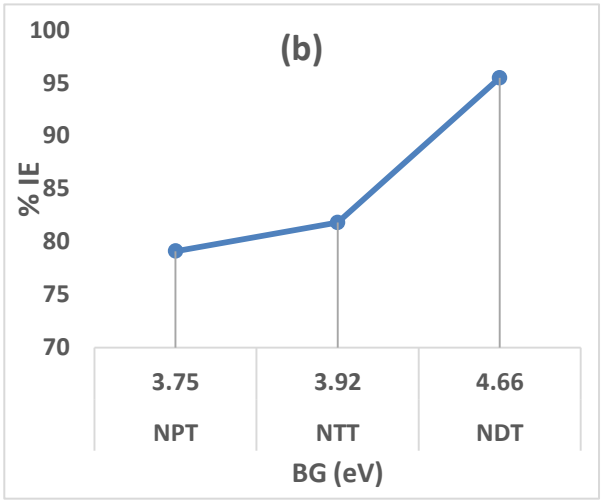
(b)
100
95
90
85
80
75
70
% IE
3.75
3.92
4.66
NPT
NTT
NDT
BG (eV)

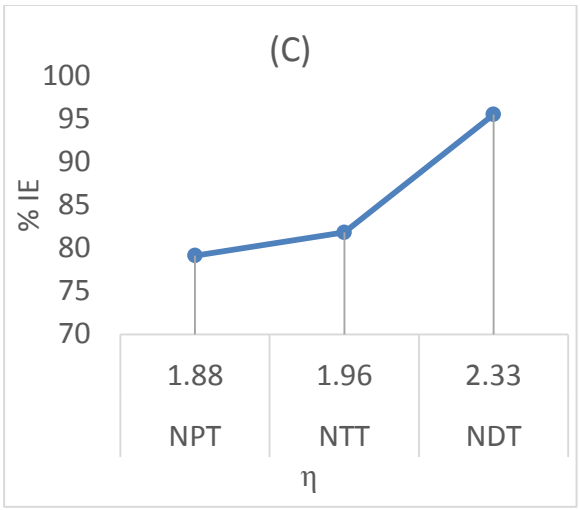
(C)
100
95
90
85
80
75
70
% IE
1.88
1.96
2.33
NPT
NTT
NDT
η

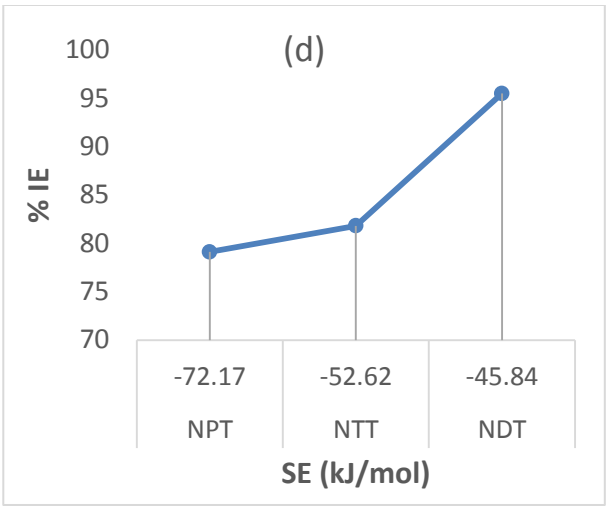
(d)
100
95
90
85
80
75
70
% IE
-72.17
-52.62
-45.84
NPT
NTT
NDT
SE (kJ/mol)

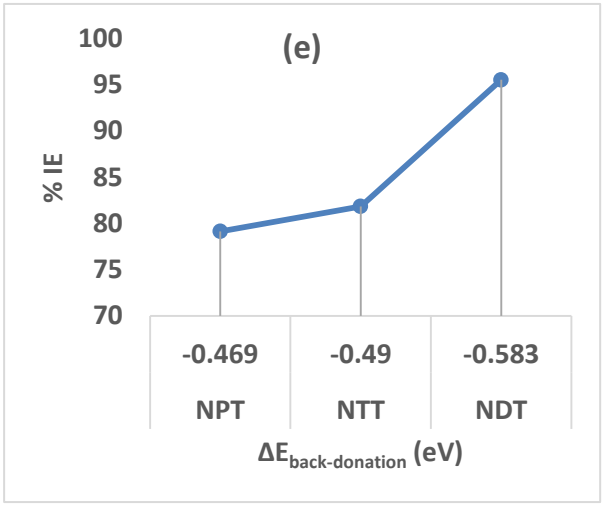
(e)
100
95
90
85
80
75
70
% IE
-0.469
-0.49
-0.583
NPT
NTT
NDT
ΔEback-donation (eV)

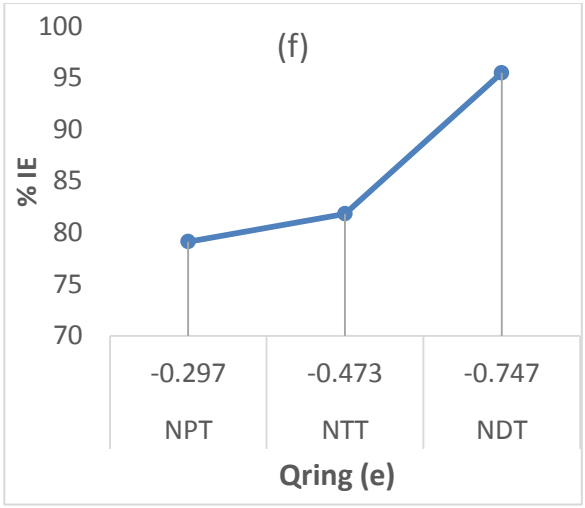
(f)
100
95
90
85
80
75
70
% IE
-0.297
-0.473
-0.747
NPT
NTT
NDT
Qring (e)

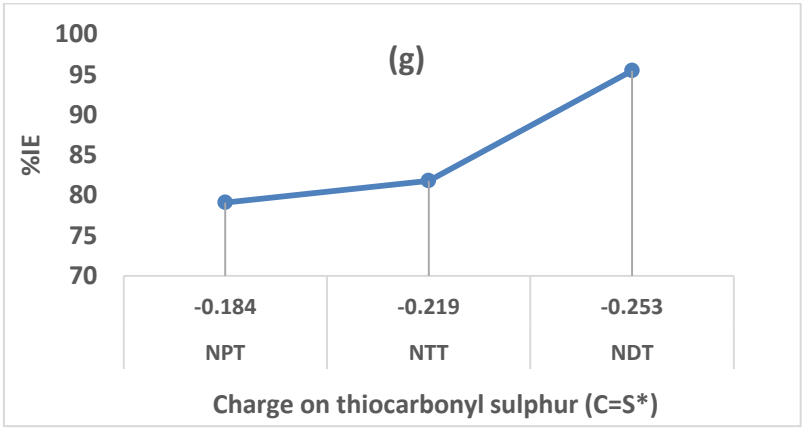

Fig. 2. Relationship between %IE and some selected descriptors: (a) Dipole Moment (DM), (b) BG = E_{HOMO}-E_{LUMO} (Band gap), (c) Chemical hardness (η), (d) Solvation energy (SE), (e) $\Delta E_{back\text{-}donation}$, (f) sum of electronic charges on rings (Q_{ring}) and (g) electric charge on thiocarbonyl sulphur (C=S* group).

Furthermore, dipole moment (DM) is an expression of non-uniform distribution of charges on various atoms in the molecule, therefore it is another important parameter to measure interactions of molecules in a particular chemical environment. It has been discussed that energy of the deformability increases with the increase in DM, making the molecule easier to be adsorbed on metal surface. Thus corrosion inhibition efficiency of a molecule increases with increasing DM [38-40]. However, it has also been argued that there is no distinct correlation between DM and inhibition efficiency [41-45]. The calculated DM values for the inhibitors in this work are inversely correlated to the observed % IE (Figure 2a).

The amount of electrons transmitted (ΔN) shows the propensity of a molecule to donate electrons and the greater the value of ΔN, the greater the propensity of a molecule to donate electrons to the electron poor species. Therefore, as corrosion inhibitors is concerned, a greater ΔN indicates a higher propensity to interrelate with the surface of the metal which will therefore leads to increasing corrosion inhibition [46,47]. Contrariwise, in this present work, there is no correlation between the trend in the ΔN values and the trend in the observed inhibition efficiency, therefore it is suggested that other means of electronic interactions apart from electron donor-acceptor model are dominant in adsorption process. Similarly, there is no distinct relationship in the chemical potential (μ), global nucleophilicity (ω) and average electronic charge on heteroatoms (Het) with observed corrosion inhibition efficiency. Nevertheless, some descriptors like $\Delta E_{back\text{-}donation}$ and dipole moment established an inverse relationship with the observed %IE (i.e. increases in value with decreasing % IE) while band gap, chemical hardness and solvation energy increases with increasing %IE as shown in Figure 2. Moreover, the quantity of calculated electron density on the rings (Q_{ring} (*e*)) and thiocarbonyl sulphur atom (C=S) in the compounds revealed that both Q_{ring} (*e*) and S* (in C=S) correlated strongly to the observed %IE (i.e. increases in value with decreasing % IE); thus ring current as well as interactions between sulphur of thiocarbonyl and metal surface plays crucial roles in the adsorption process. Therefore, the adsorption process would be typical physisorption aided by electrostatic

and π-cationic interactions rather than chemisorption as reported by Uday et al., 2013 [22]. The adsorption process is expected to be accompanied by low activation energy (E_a < 40 kcal/mol) as reported [22].

The Fukui functions permit the prediction of centre of nucleophilic (f_k^+) and electrophilic (f_k^-) attacks using density functional theory are displayed in Tables 2, 3 and 4. This is also used to reveal atoms in a molecule that have higher tendency to either donate or accept an electron. For NPT, the highest value for $f_k^+$is located on N_1 (0.014) and this depicts most apparent nucleophilic attack center, whereas the utmost value for f_k^- is found on C_2 (0.003) which shows most apparent electrophilic attack center (Table 2). For NTT, the utmost apparent centers for nucleophilic (f_k^+) and electrophilic (f_k^-) attacks are N_1 (0.013) and C_9 (0.024) respectively (Table 3). Likewise, for NDT, the highest charge for f_k^+ is found on C_3 (0.019, but f_k^- are located on three atoms in NDT namely; O_1 (0.018), C_2 (0.019) and C_3 (0.024) as shown in Table 4. Therefore, from local reactivity predictions, the electrophilic interactions of most probable atoms in NDT and metal surface showed that ring atoms in NDT actually involved in adsorption process. This is in concordance with electron density on the ring (Q_{ring} (*e*)) and thiocarbonyl sulphur atom (C=S) calculated for the compound; thus the high inhibitory efficiency exhibited by NDT could be linked to π-cationic and electrostatic interactions between the molecule and metal surface.

Table 2. The Fukui functions for NPT

Atom	$P_{N+1(r)}$	$P_{N-1(r)}$	$P_{N(r)}$	f_k^+	f_k^-
S1	-0.379	0.07	-0.184	-0.195	-0.254
N1	-0.579	-0.590	-0.593	**0.014**	-0.003
N2	-0.623	-0.591	-0.617	-0.006	-0.026
N3	-0.674	-0.590	-0.658	-0.016	-0.068
O1	-0.529	-0.419	-0.451	-0.078	-0.032
C1	-0.112	-0.084	-0.089	-0.023	-0.005
C2	-0.026	0.029	0.032	-0.058	**0.003**
C3	-0.140	-0.120	-0.123	-0.017	-0.003
C4	-0.095	-0.086	-0.090	-0.005	-0.004
C5	-0.112	-0.067	-0.076	-0.036	-0.009
C6	-0.095	-0.088	-0.092	-0.003	-0.004
C7	0.499	0.583	0.573	-0.074	-0.010
C8	0.310	0.328	0.303	0.007	-0.025
C9	0.305	0.344	0.343	-0.038	-0.001
C10	0.267	0.295	0.284	-0.017	-0.011
C11	-0.138	-0.114	-0.129	-0.009	-0.015
C12	-0.701	-0.062	-0.067	-0.634	-0.005
C13	-0.139	-0.108	-0.131	-0.008	-0.023
C14	-0.126	-0.087	-0.119	-0.007	-0.032

Table 3. The Fukui functions for NTT

Atom	$P_{N+1(r)}$	$P_{N-1(r)}$	$P_{N(r)}$	f_k^+	f_k^-
S1	-0.408	0.055	-0.219	-0.189	-0.274
S2	-0.245	0.438	0.313	-0.558	-0.125
N1	-0.559	-0.565	-0.572	**0.013**	-0.007
N2	-0.541	-0.484	-0.542	0.001	-0.058
N3	-0.471	-0.385	-0.445	-0.026	-0.060
O1	-0.599	-0.505	-0.520	-0.079	-0.015
C1	-0.112	-0.079	-0.087	-0.025	-0.008
C2	0.045	0.042	0.043	0.002	0.001
C3	-0.145	-0.119	-0.121	-0.024	-0.002
C4	-0.095	-0.085	-0.091	-0.004	-0.006
C5	-0.107	-0.062	-0.072	-0.035	-0.010
C6	-0.096	-0.088	-0.092	-0.004	-0.004
C7	0.495	0.593	0.585	-0.090	-0.008
C8	0.279	0.314	0.283	-0.004	-0.031
C9	0.303	0.307	0.331	-0.028	**0.024**
C10	-0.337	-0.255	-0.319	-0.018	-0.064
C11	0.108	0.152	0.115	-0.007	-0.037

Table 4. The Fukui functions for NDT

ATOM	$P_{N+1(r)}$	$P_{N-1(r)}$	$P_{N(r)}$	f_k^+	f_k^-
S1	-0.531	0.081	-0.253	-0.278	-0.334
N1	-0.524	-0.518	-0.527	0.003	-0.009
N2	-0.404	-0.364	-0.380	-0.024	-0.016
O1	-0.537	-0.445	-0.427	-0.110	**0.018**
C1	-0.393	-0.410	-0.405	0.012	0.005
C2	-0.070	-0.123	-0.104	0.034	**0.019**
C3	-0.096	-0.139	-0.115	**0.019**	**0.024**
C4	0.138	0.137	0.128	0.010	-0.009
C5	-0.088	-0.057	-0.084	-0.004	-0.027
C6	-0.093	-0.093	-0.102	0.009	-0.009
C7	0.517	0.553	0.556	-0.039	0.003
C8	-0.117	-0.102	-0.113	-0.004	-0.011
C9	0.213	0.282	0.282	-0.069	0.000
C10	-0.091	-0.079	-0.088	-0.003	-0.009
C11	-0.100	-0.085	-0.093	-0.007	-0.008
C12	0.088	0.070	0.081	0.007	0.011
C13	-0.085	-0.076	-0.081	-0.004	-0.005
C14	-0.111	-0.104	-0.102	-0.009	0.002
C15	-0.125	-0.118	-0.122	-0.003	-0.004
C16	-0.097	-0.077	-0.085	-0.012	-0.008
C17	-0.093	-0.077	-0.086	-0.007	-0.009

QSAR Model Using Multiple Linear Regressions

The correlation between %IE and the LUMO (0.677), band gap (1.00), η (1.00) as well as solvation energy (0.801) are positively allied, while %IE together with DM (-0.755), ω (-0.595), Het (-0.779) and ΔN (-0.595) are negatively allied. Also, most of the molecular descriptors are fairly interrelated to one another; those that are positively correlated are dipole moment and HOMO by 0.877; band gap and LUMO by 0.661; μ and HOMO by 0.814 as well as μ and LUMO by 0.888. Furthermore, SE is positively correlated with BG and η by 0.814 and 0.808 respectively; and negatively correlated with HOMO and DM by -0.839 and -0.997 respectively. Likewise, η is positively correlated with the LUMO by 0.667; Het and ω are correlated by 0.968; ΔN is positively correlated with the HOMO, DM and μ by 0.960, 0.976 and 0.619 respectively, but negatively correlated with BG, η and SE by -0.613, -0.606 and 0.958 respectively.

Similarly, η and DM are negatively correlated by -0.764; ω is negatively correlated with HOMO, LUMO, BG, μ and η by -0.548, -0.994, -0.577, -0.932 and -0.585 respectively. Also, Het shows negative relationship with LUMO, BG, μ and η by -0.989, -0.765, -0.810 and -0.771 respectively (Table 5). Therefore, the choice of effective molecular descriptors for valid analysis is a function of Pearson correlation, though the making of reliable model involved huge quantity of molecules. Additionally, the inhibitory activity of three experimental molecules is poked into and two molecular descriptors are chosen among the calculated molecular descriptors so as to evade multi-collinearity as shown in Equation 8. Also, Figure 2 shows the effectiveness of the established QSAR model as experimental %IE are well reproduced.

As shown in Table 5, the %IE values established with the help of QSAR model are replicative of the experimental %IE with fitting factor (R^2) is 1.00. This explains that the QSAR model reproduces the observed %IE of the studied compounds. Moreover, the calculated regression parameters (R^2, $CV.R^2$) for the studied molecules in an attempt to validate the developed QSAR model for inhibitory activity are shown in Table 5. The R^2 (1.00) reveals the promising fitness of the developed QSAR model (Equation 8), also the $CV.R^2$ value calculated is very close to 1.00 which is greater 0.6 [48]. This shows the model reliability and acceptability; therefore, the developed QSAR model has a promising prognostic power.

Table 5. Pearson's correlation matrix for descriptors

	%IE	HOMO	LUMO	DM	BG	μ	η	ω	Het	SE	ΔN
%IE	1.000										
HOMO	-0.346	1.000									
LUMO	0.677	0.456	1.000								
DM	-0.755	0.877	-0.029	1.000							
BG	1.000	-0.367	0.661	-0.770	1.000						
μ	0.263	0.814	0.888	0.434	0.242	1.000					
η	1.000	-0.359	0.667	-0.764	1.000	0.250	1.000				
ω	-0.595	-0.548	-0.994	-0.077	-0.577	-0.932	-0.585	1.000			
Het	-0.779	-0.319	-0.989	0.177	-0.765	-0.810	-0.771	0.968	1.000		
SE	0.801	-0.839	0.101	-0.997	0.814	-0.367	0.808	0.005	-0.248	1.000	
ΔN	-0.595	0.960	0.188	0.976	-0.613	0.619	-0.606	-0.291	-0.040	-0.958	1.000
Regression equation for anticorrosion activity										R^2	$CV. R^2$
%IE = 89.207-26.136(Het) - 44.349(ΔN) ---------- 8										1.00	0.999

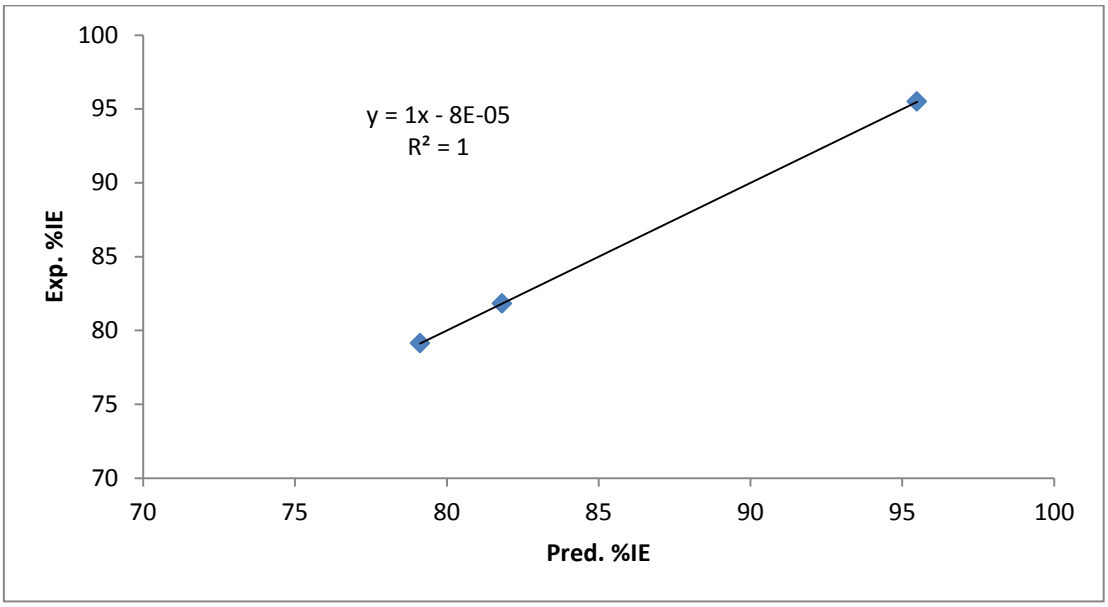

Figure 2. Correlation between experimental and predicted % IE

CONCLUSION

The molecular descriptors such as the HOMO, LUMO, dipole moment, band gap, chemical potential, chemical hardness as well as local reactivity indices have been calculated using Density Functional Theory (B3LYP/6-31G**) method for N-aroyl-N'-aryl thiourea derivatives (NDT, NTT and NPT). The calculation results revealed:

(1) That $\Delta E_{back\text{-}donation}$ and dipole moment showed an inverse relationship with the observed %IE, while band gap, chemical hardness and solvation energy increased with increasing %IE.

(2) The electron density on the rings (Q_{ring} (*e*)) and thiocarbonyl sulphur atom (S* in C=S) in the studied compounds correlated strongly with the observed %IE; thus ring current and sulphur of thiocarbonyl interactions with metal surface are crucial to the adsorption process.

(3) Therefore, it can be suggested that electronic interactions like π-cationic and n-cationic interactions will be dominant in adsorption process than electron donor-acceptor model as reported by Uday et al., 2013 [22]; thus the adsorption process should be physisorption rather than chemisorption.

(4) The electron density on the rings (Q_{ring} (*e*) calculated for NDT revealed that high inhibitory efficiency exhibited by NDT can be linked to π-cationic interactions between the molecule and metal surface.

REFERENCE

[1] M. Bouayed, H. Rabaa, A. J.Y. Srhiri, Saillard, A. Ben Bachir, Corros. Sci. 41 (1999) 501-517.

[2] P.L. Cabot, F.A. Centellas, J.A. Garrido, E. Perez, H. Vidal, Electrochim Acta, 36 (1991) 171–87.

[3] B. Semire, and A.K. Oyebamiji, New York Science Journal, 10(12) (2017) 11-21.

[4] P.A. Schweitzer, Fundamentals of metallic corrosion: atmospheric and media corrosion of metals. CRC Press, Taylor & Francis Group, second ed., 2007.

[5] C. Umezurike, J. Corr. Sci. (NICA). (1998) 73-78.
[6] V.O. Nwoko, L.E. Umoru, J. Corr. Sci. (NICA), (1998) 61-65.
[7] E. Osarolube, Nig. J. Phys. 10 (1998) 133-136.
[8] D.S. Clark, W.R. Varney, Physical Metallurgy for Engineers. Van Nostrand Reinhold Ltd., Canada, 300-315 1987.
[9] P.A. Schweitzer, Fundamentals of metallic corrosion: atmospheric and media corrosion of metals. CRC Press, Taylor & Francis Group, second ed. 2007.
[10] P.O. Ameh, N.O. Eddy, Res Chem Interme. 40(8) (2014) 2641–9.
[11] M.G. Hosseini, M. Ehteshamzadeh, T. Shahrabi, Electrochim Acta, 52 (2007) 3680.
[12] M.M. El-Naggar, Corros. Sci. 49 (2007) 2226.
[13] V.S. Sastry, Corrosion Inhibitors. Principles and Applications, John Wiley & Sons, New York, 1998.
[14] F. Bentiss, and M. Lagrenée, Journal of Material Environmental Science. 2(1) (2011) 13-17.
[15] P.C. Okafor, E.E. Ebenso, and U.J. Ekpe, International journal of electrochemical science. 5 (2010) 978-993.
[16] K.F. Khaled, Corros Sci. (2010) 2905–2916.
[17] L. Lukovitis, A. Shaban, E. Kalman, Russ J Electrochem. 19(2) (2003) 177–81.
[18] B. Semire, and A.O. Odunola, Khimiya. 22(6) (2013) 893-906.
[19] M.O. Abdulazeez, A.K. Oyebamiji, and B. Semire, Lebanese Journal of Science. 17(2) (2016) 217-232.
[20] C. Hansch, Accounts of Chemical Research. 2 (1969) 232-239.
[21] C.A. Ramsden, Quantitative Drug Design of comprehensive Medicinal Chemistry", Oxford, Vol. 4., 1990.
[22] H.R.A. Uday, M.H.A. Suaad, and A.S.A. Khulood, Journal of Al-Nahrain University. 16(4) (2013) 80-93.
[23] Spartan user's guide, Wave function, Inc, Irvine, CA 92612 USA.
[24] A.D. Becke, J. of phy Chem., 98 (1993) 5648 – 5652.
[25] L. Yang, J. Feng, and A. Ren, Polymer, 46 (2005) 10970-10982.
[26] R.G. Parr, R.A. Donnelly, M. Levy, and W.E. Palk, J. Chem. Phys. 68 (1978) 3801.
[27] D. Jacquemin, E.A. Perpete, I. Ciofini, C. Adamo, Accounts of chemical Research, 42 (2008) 326 – 3344.
[28] O.R. Khalifa, Abdallah, Elecrochim Acta, 629 (2011) 47-56.
[29] C. Lee, W. Yang, R.G. Parr, Phys. Rev. B. 37 (1988) 785.
[30] A. Becke, Journal of Physical Chemistry. 98 (1993) 5648 – 5652.
[31] A. Perez, F.J. Luque, M. Orozco, J. Am. Chem. Soc. 129 (2007) 14739-1474.
[32] B. Gomez, N.V. Likhanova, M.A. Dominguez-Aguilar, R. Martinez-Palou, R. Vela, and J. Gasquez, J. Phy. Chem B. 110 (2006) 8928-8934.
[33] Z. Zhou, and H.V. Navangul, J. Phys. Org. Chem. 3 (1990) 784-788.
[34] M. Bouachrine, M. Hamidi, S.M. Bouzzine, and H. Taoufik, J of Chem Res. 10 (2009) 29-37.
[35] L. Yang, J. Feng, and A. Ren, Polymer. 46 (2005) 10970-10982.
[36] R. Hasanov, S. Bilge, S. Bilgic, G. Gece, and Z. Kilic, Corros. Sci. 52(3) (2010) 984-990.
[37] (a) P. Udhayakala, T.V. Rajendiran, & S. Gunasekaran, J. Adv. Scient. Res. 3 (2012) 37-44. (b) P. Udhayakala, T.V. Rajendiran, & S., Gunasekaran, J. Comput. Methods Mol. Des., 2 (2012) 1-15.

[38] H. Ma, S. Chen, Z. Liu, Y. Sun, J. Mol. Struct. (Theochem), 774 (2006) 19–22.
[39] G. Gao, C. Liang, Electrochim. Acta., 52 (2007) 4554–4559.
[40] M. Lebrini, M. Lagrenée, M. Traisnel, L. Gengembre, H. Vezin, F. Bentiss, Appl. Surf. Sci. 253 (2007) 9267–9276.
[41] L.M. Rodrigez-Valdez, A. Martinez-Villfane, and D. Glossman-Mitnik, J. Mol. Struct. (THEO CHEM), 713 (2005) 65-70.
[42] A. Stoyanova, G. Petkova, and S.D. Peyerimhoff, Chem. Phys. 279 (2002) 1-6.
[43] P. Udhayakala, J. Chem. Pharm. Res. 6(7) (2014) 117-127.
[44] N.O. Eddy, F.E. Awe, C.E. Gimba, N.O. Ibisi, and E.E. Ebenso, Int. Journal of Electrochem. Sci. 6 (2011) 931-957.
[45] A.W. Nuha, M.M. Fatma, Open Journal of Physical Chemistry. 4 (2014) 6-14.
[46] B. Gomez, N.V. Likhanova, M.A. Dominguez-Aguilar, R. Martinez-Palou, A. Vela, and J. Gasquez, J. Phys. Chem., 110(18) (2006) 8928.
[47] K. Fukui, T. Yonezewa, and H. Shingu, J. Chem. Phys. 20(4) (1952) 722.
[48] P.Y. Marrero, Castillo, J. A. Garit, F. Torrens, Z.V. Romero, and E.A. Castro, Molecules. 9(12) (2004) 1100–1123.